6362 *Inorg. Chem.* **2009**, *48*, 6362–6370
DOI: 10.1021/ic802102k

Inorganic Chemistry
Article

Oxygen−Cobalt Chemistry Using a Porphyrinogen Platform

Dibyendu Bhattacharya, Suman Maji, Kuntal Pal, and Sabyasachi Sarkar*

Indian Institute of Technology Kanpur, Kanpur 208016, India

Received June 28, 2008

The tetraethylammonium salt of the Co(II)porphyrinogen complex, $[Et_4N]_2[LCo(II)]$, **1**, (L = tetrakis(cyclohexyl)-porphyrinogen tetraanion) is oxidized by atmospheric oxygen to form $[Et_4N][LCo(III)]$, **2**, in contrast to the ligand oxidation of Co(II)porphyrinogen, $[Li(THF)_2]_2[L'Co(II)]$ (L′ = octaethylporphyrinogen tetraanion) with pure oxygen (Angelis, S. D.; Solari, E.; Floriani, C.; Chiesi-Villa, A.; Rizzoli, C. *J. Am. Chem. Soc.* **1994**, *116*, 5702). Substitution of the η^4-bound lithium cation ($[Li(THF)_2]^+$) on the periphery of the pyrollyl ring of $[Li(THF)_2]_2[L'Co(II)]$ with a tetraethylammonium cation ($[Et_4N]^+$) resulted in a metal-centered redox reaction analogous to that of **1** with oxygen, and thus demonstrated that the difference in reactivity is due to the change in the countercation rather than the substitution of the peripheral ligand. Reaction of $[Et_4N][LCo(III)]$, **2**, with elemental iodine produced $[L^{\Delta\Delta}Co(II)\text{-}I](I_3)(I_2)$, **3**. This reaction is viewed as an iodine-induced electron transfer reaction across Co(III)−porphyrinogen, in which the four electrons that originated from the oxidation of the internal reductant (porphyrinogen) to porphodimethene are shared by the internal oxidant (Co(III)), and the external oxidant (iodine), resulting in the reduction to Co(II) and iodide, respectively. Complexes **2** and **3** were characterized by spectroscopic studies, cyclic voltammetry (CV), magnetic moment measurements, and by single-crystal X-ray diffraction studies. The structural properties of **2** were analyzed based on the density functional theoretical (DFT) framework.

Introduction

The reactivity of cobalt-ammine complexes with atmospheric oxygen was investigated independently by Jörgenson and Werner[1] in the dawning era of coordination chemistry. Such a reaction of cobalt(II), in the presence of an ammine ligand, with air is known to produce a superoxo-bridged dimeric Co(III) complex where the unpaired electron is delocalized over the $\{Co(\mu-O_2)Co\}$ moiety.[2] However, the Schiff base derived mononuclear cobalt complexes form adducts with oxygen possessing either $\{Co(II)\text{-}O_2\}$ or $\{Co(III)\text{-}O_2^{\bullet-}\}$ moiety, which mimics the interaction between dioxygen and hemoglobin. In the presence of pyridine and oxygen, a Schiff base Co(II) complex readily forms a complex like $[Co(bzacen)py\cdot O_2]$ (bzacen = bis(benzoylacetone)ethylenediamine), possessing a Co(III) center with a terminal O_2^- coordination. Direct synthesis and structural characterization of this complex as a Co(III) species coordinated with O_2^- supports such coordination.[3] These products have been studied extensively as models for naturally occurring oxygen-transport proteins.[4] Thus, when cobalt(II) reacts with dioxygen, the cobalt−oxygen bond either forms as a peroxo- or superoxo-bridged species or remains as a monomer with an end-on superoxide linkage. In these reactions the electron transfer between Co(II) and molecular oxygen requires direct {Co−O} bond formation, as shown in eq 1:

$$2Co(II)+O_2 \leftrightarrow \{CoO_2\}+Co(II) \leftrightarrow \{CoO_2Co\} \rightarrow 2Co(III) \quad (1)$$

Porphyrinogen, the precursor of porphyrin,[5] with potential four N-atom donor sites, is unstable to respond in the dehydrogenase reaction.[6] However, the synthesis of

*To whom correspondence should be addressed. E-mail: abya@iitk.ac.in. Fax: +91(512)2597265.

(1) (a) Jörgensen, S. M. *J. Prakt. Chem.* **1886**, *33*, 489. (b) Werner, A. *Z. Anorg. Chem.* **1893**, *3*, 267. (c) Werner, A. *Ber.* **1906**, *39*, 2673. (d) Werner, A. *Ber.* **1907**, *40*, 4098. Cited in:(e) Moeller, T. *Inorganic Chemistry, An Advanced Text Book*; Wiley: New York, 1952; Chapter 7, pp 251−265.

(2) (a) Dhanasekaran, T.; Natarajan, P. *J. Am. Chem. Soc.* **1992**, *114*, 4621. (b) Harris, W. R.; McLendon, G. L.; Martell, A. E.; Bess, R. C.; Mason, M. *Inorg. Chem.* **1980**, *19*, 21. (c) Tanase, T.; Onaka, T.; Nakagoshi, M.; Kinoshita, I.; Shibata, K.; Doe, M.; Fujii, J.; Yano, S. *Inorg. Chem.* **1999**, *38*, 3150. (d) Chufn, E. E.; Verani, C. N.; Puiu, S. C.; Rentschler, E.; Schatzschneider, U.; Incarvito, C.; Rheingold, A. L.; Karlin, K. D. *Inorg. Chem.* **2007**, *46*, 3017.

(3) Ellis, J.; Pratt, J. M.; Green, M. *J. Chem. Soc., Chem. Commun.* **1973**, 781.

(4) (a) Collman, J. P.; Gagne, R. R.; Halbert, T. R.; Marchon, J.-C.; Reed, C. A. *J. Am. Chem. Soc.* **1973**, *95*, 7868. (b) Molinaro, F. S.; Little, R. G.; Ibers, J. A. *J. Am. Chem. Soc.* **1977**, *99*, 5628. (c) Momenteau, M.; Lavalette, D. *J. Chem. Soc., Chem. Commun.* **1982**, 341. (d) Yang, J.; Huang, P. *Chem. Mater.* **2000**, *12*, 2693. (e) Stynes, D. V.; Stynes, H. C.; James, B. R.; Ibers, J. A. *J. Am. Chem. Soc.* **1973**, *95*, 1796. (f) Basolo, F.; Hoffman, B. M.; Ibers, J. A. *Acc. Chem. Res.* **1975**, *8*, 384.

(5) (a) Viale, L. C. S. M. D.; Molina, M. D. C. R. D.; Calmanovici, R. W. D.; Tomio, J. M. *Biochem. J.* **1977**, *168*, 393. (b) Li, F.; Lim, C. K.; Peters, T. J. *Biochem. J.* **1987**, *243*, 621.

(6) Elder, G. H. In *Iron in Biochemistry and Medicine II*; Jacobs, A., Worwood, M., Eds.; Academic Press: London, 1980; pp 245−292.

 Published on Web 06/17/2009

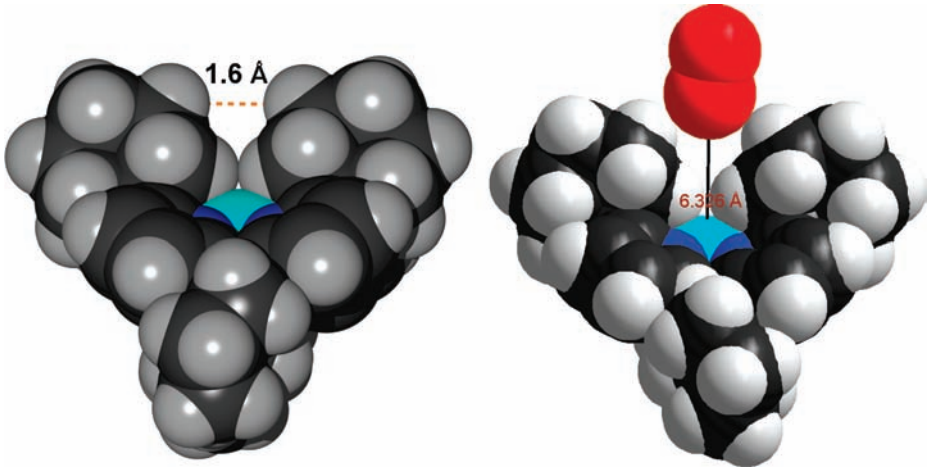

Figure 1. Space filling model of **2** indicating no room for direct interaction with central cobalt metal. Oxygen molecule (red color) indicates close possible approach to the metal center.

porphyrinogen[7a] prototypes has been achieved with a few modifications.[7b−7e] The interactions of these porphyrinogen prototypes with transitional metals have been studied extensively by Floriani et al.[8a−8e] and by others.[8f−8j] Octaethyl- and octamethyl porphyrinogens, in which alkyl substitutions of the *meso* hydrogens prevented an exhaustive dehydrogenase-type reaction, are the most thoroughly studied synthetic porphyrinogens.

Most of these complexes have been isolated as $[Li(THF)_2]_2[L'M(II)]$ (M = transition metal, L′ = octaalkylporphyrinogen tetraanion). Structural studies of these complexes show that the $[Li(THF)_2]^+$ part in these complexes is present not only as a cation but this is strongly coordinated with porphyrinogen in an η^4-fashion. Such association of the cation beyond the ionic interaction may influence the redox behavior of the complexed anion, $[L'M(II)]^{2-}$. Interestingly, the redox chemistry of metalated porphyrinogens is diverse and varied. Curiously, copper(II) chloride oxidizes species like $[Li(THF)_2]_2[L'Co(II)]$ (L′ = *meso*-octaethylporphyrinogen tetraanion) to newer derivatives with unprecedented metal cluster counterions.[8d] Surprisingly, $[Li(THF)_2]_2[L'Co(II)]$ reacts with molecular oxygen, resulting in two-electron oxidation of the coordinated porphyrinogen to porphomethene in 20% yield without affecting the oxidation state of the coordinated Co(II).[8e] Thus, the diverse redox activities of the metalloporphyrinogens may result from either the central metal or the coordinated ligand, and sometimes may happen from both. Therefore, such diverse possibilities of electron transfer reaction may be relevant with cobalt coordinated to macrocycle ligand like corrin as in the cofactor, cobalamin. The formation of superoxide species by the interaction of Co(II) and aerial oxygen in the presence of nitrogen donor ligand may relate the cobalamin-dependent enzymatic reactions which are of a radical type[9] and are directly related to oxidative stress.

Cobalt(II) with N donor ligands, is generally oxidized by oxygen to yield Co(III). Therefore, the retention of the oxidation state of Co(II) in the reaction of $[Li(THF)_2]_2[L'Co(II)]$ with oxygen is unique[8e] and requires further investigations. We substituted the countercation, $[Li(THF)_2]^+$, with a quaternary ammonium ion, which led to smooth oxidation of the central Co(II) to Co(III) to yield $[Et_4N][LCo(III)]$, **2**. This reaction was extended to $[Et_4N]_2[L'Co(II)]$, and in contrast to the reaction of $[Li(THF)_2]_2[L'Co(II)]$ with oxygen, smooth cobalt centered oxidation occurred to yield $[Et_4N][L'Co(III)]$. It is now evident that the introduction of the $[Et_4N]^+$ cation results in a metal-centered oxidation reaction. In this type of redox reaction, a one-electron reduction of molecular oxygen occurs with the concurrent formation of a superoxide radical ion, as has been reported for Cu(II)porphyrinogen.[8j] Using a one-electron oxidant, such as the kinetically inert $[Cp_2Fe(III)][PF_6]$, (Cp = cyclopentadenyl), the oxidation of **1** to **2** is achieved, demonstrating that such oxidation occurs from an outer-sphere electron-transfer reaction. This reaction mechanism is also supported by analysis of a space-filling model, which shows that direct bonding of oxygen to the central cobalt is difficult because of steric crowding, which prevents the formation of any precursor $\{Co-O_2\}$ complex (Figure 1). The Co(III) complex thus formed further participates in a reaction with iodine, in which iodine acts as the external oxidant and Co(III) functions as the internal oxidant, concomitant with the oxidation of the coordinated porphyrinogen ligand (reductant) to porphodimethene, thus constituting an induced electron transfer reaction.

Experimental Section

Materials. All reactions and manipulations were performed under a pure argon atmosphere using a modified Schlenk and vacuum-line technique. Solvents, pyrrole, and cyclohexanone were obtained from S. D. Fine Chemicals Ltd. India, and were purified and dried before use by standard methods. Et_4NCl and iodine were obtained from Acros Organics. The $[Cp_2Fe(III)][PF_6]$ used in this

(7) (a) Bayer, A. *Chem. Ber.* **1816**, *19*, 2184. (b) Dennstedt, M.; Zimmermann, J. *J. Chem. Ber.* **1890**, *23*, 1370. (c) Chelintzev, V. V.; Tronov, B. V. J. *Russ. Phys. Chem. Soc.* **1916**, *48*, 105. (d) Rothemund, P.; Gage, C. L. *J. Am. Chem. Soc.* **1955**, *77*, 3340. (e) Dey, S.; Pal, K.; Sarkar, S. *Tetrahedron Lett.* **2006**, *47*, 5851.

(8) (a) Jacoby, D.; Floriani, C.; Chiesi-Villa, A.; Rizzoli, C. *J. Chem. Soc., Chem. Commun.* **1991**, 220. (b) Jubb, J.; Jacoby, D.; Floriani, C.; Chiesi-Villa, A.; Rizzoli, C. *Inorg. Chem.* **1992**, *31*, 1306. (c) Jubb, J.; Floriani, C.; Chiesi-Villa, A.; Rizzoli, C. *J. Am. Chem. Soc.* **1992**, *114*, 6571. (d) De Angelis, S.; Solari, E.; Floriani, C.; Chiesi-Villa, A.; Rizzoli, C. *J. Am. Chem. Soc.* **1994**, *116*, 5691. (e) De Angelis, S.; Solari, E.; Floriani, C.; Chiesi-Villa, A.; Rizzoli, C. *J. Am. Chem. Soc.* **1994**, *116*, 5702. (f) Bachmann, J.; Nocera, D. G. *J. Am. Chem. Soc.* **2004**, *126*, 2829. (g) Bachmann, J.; Nocera, D. G. *J. Am. Chem. Soc.* **2005**, *127*, 4730. (h) Bachmann, J.; Hodgkiss, J. M.; Young, E. R.; Nocera, D. G. *Inorg. Chem.* **2007**, *46*, 607. (i) Bhattacharya, D.; Dey, S.; Maji, S.; Pal, K.; Sarkar, S. *Inorg. Chem.* **2005**, *44*, 7699. (j) Bhattacharya, D.; Maji, S.; Pal, K.; Sarkar, S. *Inorg. Chem.* **2008**, *47*, 5036.

(9) (a) Banerjee, R. *Biochem.* **2001**, *40*, 6191. (b) Matthews, R. G. *Acc. Chem. Res.* **2001**, *34*, 681.

work was freshly synthesized by dissolving [Cp_2Fe(II)] in concentrated sulfuric acid followed by oxidation in air. The resulting deep violet solution was diluted with water, and the blue-violet oxidized species was precipitated as [Cp_2Fe(III)][PF_6] by addition of a concentrated aqueous solution of NH_4PF_6.

Physical Measurements and Procedures. Electronic absorption spectral measurements were made using a USB 2000 UV−visible spectrophotometer (Ocean Optics Inc.) equipped with fiber optics. Infrared spectra were recorded using pressed KBr disks on a Bruker Vertex 70, FT-IR spectrophotometer. Analysis for carbon, hydrogen and nitrogen were carried out with a Perkin-Elmer 2400 microanalyzer. Iodine was estimated gravimetrically as AgI using standard analytical methods. Cyclic voltammetric measurements were performed with BASi Epsilon- EC Bioanalytical Systems Inc. Cyclic voltammograms were recorded using a glassy carbon electrode as the working electrode, Pt wire as the auxiliary electrode, and an Ag/AgCl electrode as the reference electrode. All electrochemical experiments were performed under an argon atmosphere at 298 K. Potentials were referenced against internal ferrocene (Fc) and are reported relative to the Ag/AgCl electrode ($E_{1/2}(Fc^+/Fc)$ = +0.49 V vs Ag/AgCl). Cyclic voltammogram (CV) and differential pulse polarographs (DPP) were obtained with 0.1 M Bu_4NClO_4 as the supporting electrolyte in dichloromethane, CH_3CN, *N*,*N*-dimethylformamide (DMF), or dimethylsulfoxide (DMSO) and with Bu_4NPF_6 as the supporting electrolyte in tetrahydrofuran (THF). The CV scan rate was 100 mV/s. Magnetic susceptibilities were measured at 0.5 T as a powder packed in gelatin capsules using a Quantum Design MPMSR2 SQUID susceptometer. The data were corrected for the diamagnetism of the sample holder, and the diamagnetic components of the sample were evaluated using Pascal's constants. X-band ESR measurements of frozen solutions were performed at 77 K using a Bruker EMX spectrometer. The conductivity measurements were performed along the *a* and *b* axes, that is, along the stacks between two planes of porphodimethene units and along the polyiodide $\cdots I_3^-\cdots I_2\cdots I_3^-\cdots I_2\cdots$ zigzag chains, using a standard four-point probe technique with a sampling current of 20 μA. A single crystal of **3** with a dimension of 1.013 mm (along the crystallographic *a* axis), 0.319 mm (along the *c* axis), and 0.159 mm (along the *b* axis) was mounted on silvered graphite fibers, and electrical contact was made using palladium paste. Variation in temperature was achieved by placing the samples in a cold-gas stream (N_2 or He). The conductivity of the material was calculated from the relationship $\sigma = L/RA$, where σ is the conductivity (in Ω^{-1} cm^{-1}), *R* is the measured resistance (in Ω) of the material between two inner contacts, *L* is the separation distance between two inner contacts (in cm), and *A* is the cross-sectional area of the sample (in cm^2). The relationship between resistance and temperature was measured using a Keithley source meter (2400).

Computational Details. All calculations were performed with the Gaussian 03, revision B.04, package.[10] Molecular orbitals were visualized using "Gauss View 3.0". Gas-phase and single-point calculations, as well as population analysis of molecular orbitals, were performed based on density functional theory (DFT). The method used was Becke's three-parameter, hybrid-exchange functional,[11] the non-local correlation was provided by the Lee, Yang, and Parr expression (B3LYP), and by the Vosko, Wilk, and Nusair (1980) correlation functional (III) for local (B3LYP). The 6-31 g(d,p) basis set[12] was used for H, C, and N atoms and MidiX was used[13] for I atoms; the LANL2DZ[14] basis set and LANL2 pseudopotentials of Hay and Wadt[15] were used for Co atoms. The geometry of **2** was obtained from its crystal structure. Because spin restriction was lifted, there was no common spatial wave function for the α and β spin pair, and the two manifolds of orbitals were drawn separately. In each case, the β spin bears a 90% d character.

Table 1. Selected Crystallographic Data for **2** and **3**

compounds	**2**	**3**
formula	$C_{51}H_{74}N_5Cl_6Co_1$	$C_{44}H_{16}N_4Cl_4I_6Co_1$
formula weight	1028.78	1575.01
T/K	100 (2) K	100 (2) K
wavelength	0.71073 Å	0.71073 Å
crystal system	orthorhombic	triclinic
space group	*P* 21 21 21	$P\bar{1}$
a / Å	13.562(5)	11.719(5)
b / Å	18.321(5)	12.962(5)
c /Å	20.330(5)	17.870(5)
α / deg	90	85.768 (5)
β / deg	90	72.840 (5)
γ / deg	90	72.228 (5)
V / Å^3	5051(3)	2469.5(16)
Z	4	2
D_c (mg.cm^{-3})	1.353	2.118
crystal color and shape	dark red, block	brown, block
crystal size (mm^3)	0.20×0.10×0.08	0.20×0.18×0.15
F(000)	2176	1490
absorption coeff.(mm^{-1})	0.698	4.349
θ range (deg) for data collection	2.12−28.29	2.02−28.27
index ranges	$-17 \le h \le 12$ $-24 \le k \le 22$ $-22 \le l \le 27$	$-15 \le h \le 14$ $-17 \le k \le 16$ $-23 \le l \le 11$
reflections collected	34126	16191
unique reflections	12250	12254
independent reflns(R_{int})	0.0450	0.0301
completeness to θ_{max}	98.7%	98.9%
data/restraints/parameters	12250/0/573	12254/0/511
GOF[c] on F^2	1.039	1.041
R1,[a] wR2[b] [$I > 2\sigma(I)$]	0.0445, 0.0925	0.0656, 0.1632
R1,[a] wR2[b] (all data)	0.0522, 0.0957	0.0847, 0.1750
largest diff. peak and hole	0.566, −0.285 e A^{-3}	0.922, −0.855 e A^{-3}
Flack parameter	0.0(5)	

[a] $R_1 = \sum||F_o|-|F_c||/\sum|F_o|$. [b] $wR_2 = \{\sum w(F_o^2-F_c^2)^2/\sum w(F_o^2)^2\}^{1/2}$.

X-ray Crystal Structure Analysis. The crystallographic data are presented in Table 1. Suitable single crystals of complexes **2** ($0.20 \times 0.10 \times 0.10$ mm^3) and **3** ($0.20 \times 0.12 \times 0.10$ mm^3) were mounted on a Siemens CCD diffractometer equipped with a graphite-monochromated Mo Kα (λ = 0.71073 Å) radiation source. The unit cell parameters and crystal-orientation matrices were determined for the two complexes by least-squares refinements of all reflections. The intensity data were corrected for both Lorentz and polarization effects, and an empirical

(10) Frisch, M. J., Trucks, G. W.; Schlegel, H. B.; Scuseria, G. E.; Robb, M. A.; Cheeseman, J. R.; Montgomery, J. A., Jr.; Vreven, T.; Kudin, K. N.; Burant, J. C.; Millam, J. M.; Iyengar, S. S.; Tomasi, J.; Barone, V.; Mennucci, B.; Cossi, M.; Scalmani, G.; Rega, N.; Petersson, G. A.; Nakatsuji, H.; Hada, M.; Ehara, M.; Toyota, K.; Fukuda, R.; Hasegawa, J.; Ishida, M.; Nakajima, T.; Honda, Y.; Kitao, O.; Nakai, H.; Klene, M.; Li, X.; Knox, J. E.; Hratchian, H. P.; Cross, J. B.; Bakken, V.; Adamo, C.; Jaramillo, J.; Gomperts, R.; Stratmann, R. E.; Yazyev, O.; Austin, A. J.; Cammi, R.; Pomelli, C.; Ochterski, J. W.; Ayala, P. Y.; Morokuma, K.; Voth, G. A.; Salvador, P.; Dannenberg, J. J.; Zakrzewski, V. G.; Dapprich, S.; Daniels, A. D.; Strain, M. C.; Farkas, O.; Malick, D. K.; Rabuck, A. D.; Raghavachari, K.; Foresman, J. B.; Ortiz, J. V.; Cui, Q.; Baboul, A. G.; Clifford, S.; Cioslowski, J.; Stefanov, B. B.; Liu, G.; Liashenko, A.; Piskorz, P.; Komaromi, I.; Martin, R. L.; Fox, D. J.; Keith, T.; Al-Laham, M. A.; Peng, C. Y.; Nanayakkara, A.; Challacombe, M.; Gill, P. M. W.; Johnson, B.; Chen, W.; Wong, M. W.; Gonzalez, C.; Pople, J. A. *Gaussian 03*, revision B.04; Gaussian, Inc.: Pittsburgh, PA, 2003.

(11) (a) Becke, A. D. *J. Chem. Phys.* **1993**, *98*, 5648. (b) Lee, C.; Yang, W.; Par, R. G. *Phys. Rev.* **1988**, *B37*, 785.

(12) Patersson, G. A.; Al-Laham, M. A. *J. Chem. Phys.* **1991**, *94*, 6081.

(13) Easton, R. E.; Giesen, D. J.; Welch, A.; Cramer, C. J.; Truhlar, D. G. *Theor. Chim. Acta* **1996**, *93*, 281.

(14) Hay, P. J.; Wadt, W. R. *J. Chem. Phys.* **1985**, *82*, 299.

(15) (a) Hay, P. J.; Wadt, W. R. *J. Chem. Phys.* **1985**, *82*, 270. (b) Wadt, W. R.; Hay, P. J. *J. Chem. Phys.* **1985**, *82*, 284.

absorption correction was also applied using the SAINT program.[16] Data were collected by applying the condition $I > 2\sigma(I)$. All structures were solved by direct methods, followed by successive and different Fourier syntheses. Full-matrix, least-squares refinements on F^2 were carried out using SHELXL-97 with anisotropic displacement parameters for all non-hydrogen atoms. Hydrogen atoms were constrained to ride on the respective carbon or nitrogen atoms with isotropic displacement parameters equal to 1.2 times the equivalent isotropic displacement of their parent atoms in all cases. Complex neutral atom scattering factors were used throughout for all cases. All calculations were carried out using SHELXS 97,[17] SHELXL 97,[18] PLATON 99,[19] and ORTEP-3[20] programs.

Synthesis. The ligands, 5,10,15,20 tetrakiscyclohexylporphyrinogen (L) and octaethylporphyrinogen (L′), were synthesized as reported earlier.[7e] The lithium salt of the ligand was synthesized using a standard procedure.[21]

Synthesis of $[Et_4N]_2[LCo(II)]$ (1). To 1.09 g (1.2 mmol) of the lithium salt of L in THF (10 mL) was added 0.14 g (1.1 mmol) of anhydrous cobaltous chloride in 3 mL of THF with stirring, after which the solution immediately turned pale brown. After stirring at room temperature (RT) for 2 h, 0.4 g (2.4 mmol) of Et_4NCl dissolved in 5 mL of dichloromethane (DCM) was added. After half an hour, excess petroleum ether was added to precipitate the desired product, which was then filtered, washed with petroleum ether and vacuum-dried. In solution, compound **1** was extremely air sensitive. Yield: 75% (1.2 g, 1.22 mmol). UV−vis $\lambda_{max/nm}$ ($\varepsilon/M^{-1}\,cm^{-1}$) in DCM: 374 (4038). IR: υ_{max} (cm^{-1}) = 3085 s (pyrrole C−H), 2920 d ($-CH_2CH_3$), 2874 s ($-CH_2CH_3$), 2214 m (C−H), 2115 m (C−H), 1571w,1540 w,1528 w,1412 s. Calcd (Found) [$C_{53}H_{79}N_6Co$(II)] C, 74.05 (73.39), H, 10.19 (10.05), N, 9.25 (9.11).

Synthesis of $[Et_4N][LCo(III)]\cdot 3CH_2Cl_2$ (2). To 1.09 g (1.2 mmol) of the lithium salt of L in THF (10 mL) was added 0.14 g (1.1 mmol) of anhydrous cobaltous chloride in 3 mL of THF with stirring, after which the solution immediately turned pale brown. After stirring at RT for 2 h, 0.2 g (1.2 mmol) of Et_4NCl dissolved in 5 mL of DCM was added. At this stage the flow of argon was stopped, and the solution was exposed to air with stirring. Within minutes, the solution changed from pale brown to bright red. After waiting for approximately 30 min for the completion of the reaction, the solution was dried under reduced pressure to yield a crude solid. After washing with 5 mL of water, isopropanol, and diethyl ether, the solid was then vacuum-dried. During washing with water, the excess unreacted metal chloride and cation were removed. The crude product was dissolved in dichloromethane and was reprecipitated by addition of diethyl ether for a yield of 80% (1.0 g, 0.98 mmol). Single crystals suitable for X-ray crystallography were obtained from a DCM/petroleum ether mixture (1:1). UV−vis $\lambda_{max/nm}$ ($\varepsilon/M^{-1}\,cm^{-1}$) in DCM: 473(3831), 734(4476). IR:υ_{max} (cm^{-1}) = 3094 s (pyrrole C−H), 2920 d ($-CH_2CH_3$), 2874 s ($-CH_2CH_3$), 2214 m (C−H), 2115 m (C−H), 1571s, 1540 s, 1528 w, 1412 s Calcd (Found) [$C_{51}H_{74}N_5Cl_6Co$(III)] C, 59.54 (58.28), H, 7.24 (7.29), N, 6.80 (6.31).

Synthesis of $[Et_4N][L'Co(III)]$. This was synthesized by following the procedure as described in the isolation of **1** but replacing L by L′. After exposure to air, the pale brown, dichloromethane solution of $[Et_4N]_2[L'Co(II)]$ was converted to a bright red solution of $[Et_4N][L'Co(III)]$. After 30 min of exposure to air, the crude product was isolated and purified as described to isolate **2**. Elemental analyses showed the electronic spectrum and magnetic properties (3.50 μ_B at 298 K) of this compound to be similar to that of **2**.

Oxidation of 1 Using $[Cp_2Fe(III)][PF_6]$. A 0.5 g portion of **1** (0.51 mmol) was dissolved in 10 mL of dichloromethane under an argon atmosphere. To the pale brown solution, 5 mL of a blue dichloromethane solution of ferrocenium hexafluorophosphate (0.17 g, 0.51 mmol) were added with stirring, whereupon the color of the solution changed to green. The green solution was stirred for 30 min for removal of the solvent by evaporation. The resulting solid was then washed with toluene to remove the ferrocene that had formed. The solid residue was then dissolved in acetone. Careful addition of water allowed fractional precipitation of the desired complex, leaving the byproduct $[Et_4N][PF_6]$ in solution. The water from the precipitate was removed by quick washing with isopropanol. In the final step of the synthesis, the product was recrystallized in a DCM/petroleum ether mixture (1:1) for a yield of 70% (0.3 g, 0.27 mmol). The elemental analyses and spectroscopic properties of this complex revealed its identity to be **2**.

Synthesis of $[L^{\triangle\triangle}Co(II)-I](I_3)(I_2)\cdot 2CH_2Cl_2$ (3). Into a DCM solution of **2** (1.0 g, dissolved in 30 mL DCM) was slowly added an iodine (1.0 g) solution in 20 mL of DCM over a period of 15 min, which caused the solution to become reddish green. The solution was filtered to remove any trace of insoluble byproduct, and 40 mL of petroleum ether were added to the filtrate. After standing at 4 °C for 6 h, shiny red crystals with a green hue appeared. The crystals were removed by filtration, and the volume of the filtrate was reduced to 30 mL. Addition of fresh petroleum ether (50 mL) to this solution precipitated a fresh crop of the microcrystalline solid, which was isolated by filtration, washed with petroleum ether, and vacuum-dried. The microcrystalline solid thus obtained was identical to the isolated crystals. Yield: 71% (1.4 g, 0.83 mmol), based on **2**. UV−vis $\lambda_{max/nm}$ ($\varepsilon/M^{-1}\,cm^{-1}$) in DCM: 293(7538), 363(38,110), 524(sh). IR: υ_{max} (cm^{-1}) = 3110 s (pyrrole C−H), 3074 s (cyclopropane C−C), 2920 ($-CH_2CH_3$), 2874 ($-CH_2CH_3$), 2214 (C−H), 2115 (C−H). Calcd (Found) [$C_{42}H_{52}N_4Cl_4I_6Co$(II)] C, 33.81 (32.87), H, 1.03 (1.12), N, 3.58 (3.39), I, 48.36 (49.20).

Results and Discussion

Synthesis. The modified procedure adopted here for the synthesis of cobalt porphyrinogens could alleviate the complications described previously[8b,8e] while sacrificing neither the yield nor the purity of the complex. The synthetic strategy is outlined in Scheme 1. Anhydrous

Scheme 1. Reaction Scheme

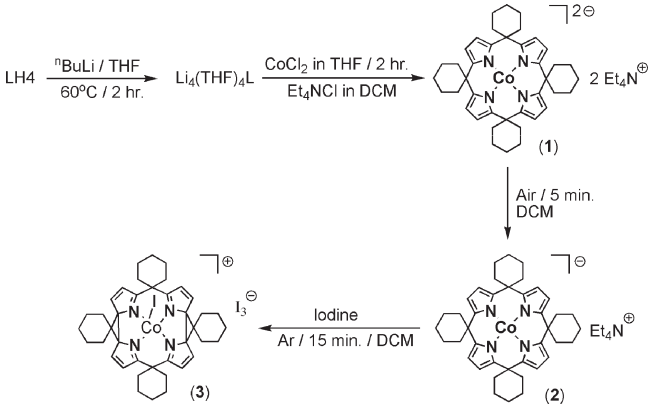

(16) *SMART and SAINT*; Bruker AXS Inc.: Madison, WI, 1998.
(17) Sheldrick, G. M. *SHELXS 97, Program for the Solution of Crystal Structure*; University of Göttingen: Göttingen, Germany, 1997.
(18) Sheldrick, G. M. *SHELXL 97, Program for the Solution of Crystal Structure*; University of Göttingen: Göttingen, Germany, 1997.
(19) Spek, A. L. *PLATON, Molecular Geometry Program*; University of Utrecht: Utrecht, The Netherlands, 1999.
(20) Farrugia, L. J. ORTEP-3 for windows. *J. Appl. Crystallogr.* **1997**, *30*. 565.
(21) (a) Jacoby, D.; Floriani, C.; Chiesi-Villa, A.; Rizzoli, C. *J. Am. Chem. Soc.* **1993**, *115*, 3595. (b) Crescenzi, R.; Solari, E.; Floriani, C.; Chiesi-Villa, A.; Rizzoli, C. *J. Am. Chem. Soc.* **1999**, *121*, 1695.

$CoCl_2$ in dry THF was allowed to react with lithium porphyrinogen at room temperature for less than 2 h with stirring, which was adequate for the complete introduction of cobalt(II) ions into the porphyrinogen core. Here the choice of solvent, THF over toluene, which was used in the earlier work,[8e] allowed completion of the reaction within hours rather than days. The desired complex, $[Et_4N]_2[LCo(II)]$ (**1**), was synthesized via a metathesis reaction in dichloromethane using tetraalkylammonium, rather than $[Li(THF)_2]^+$, as the countercation. Complex **1** was air sensitive both in solution and in the solid state. This reaction scheme was extended to the direct synthesis of $[Et_4N]_2[L'Co(II)]$ without isolation of the reported intermediate complex, $[Li(THF)_2]_2[L'Co(II)]$.[8e]

Oxidation of **1** to realize the compound $[Et_4N][LCo(III)]$ (**2**) was similar to the oxidation of cobalt-ammine complexes in air, as described by Jörgenson and Werner.[1] However, in the present case, the oxidation in air may not be leading to a direct interaction between the cobalt center and the oxygen as envisaged in eq 1. This can be seen in the facile oxidation of **1** to **2** using $[Cp_2Fe(III)][PF_6]$, which suggests an outer-sphere, electron-transfer reaction mechanism. The one-electron redox product resulting from the conversion of **1** to **2** was identified as a superoxide ion using the NBT formazan assay, as discussed later.

The four-electron oxidation of a metalloporphyrinogen by the Cu(II) ion to a metalloporphodimethene, which results in the formation of copper cluster anions as a byproduct, has been extensively studied.[8d,8e] A similar oxidation reaction, in which the Cu(II) ion was replaced with a ferrocenium cation, has been reported.[8g] Previously, we used iodine as an oxidant to isolate metalloporphodimethene.[8i] In the present study, we extended the oxidation by iodine to the isolation of the cobalt(II)porphodimethene complex. Interestingly, a four-electron reduction of $L^{\Delta\Delta}$ to L^{4-} using iodide as the reductant has been reported previously.[8h] Such reactions in opposing directions apparently question the spontaneity of these reactions in both of the directions. The use of iodine as the oxidant to oxidize the coordinated porphyrinogen to porphodimethene with the apparent reduction of the metal center by one electron and the formation of conjugate reductant iodide seem to conflict with reports of the reverse reaction using iodide as the reductant. Typically, porphyrinogens are expected to undergo a pair of successive, two-electron oxidations. This reaction is known to occur for metalloporphyrinogens with redox inactive zinc[8f] and also with redox active iron[8g] complexes. These reactions established that the ligand-based dehydrogenase-type reaction is possible with these porphyrinogens when a coordinated redox active metal participates in the redox reaction. In this context, the reaction between $[L'^{\Delta\Delta}Fe(II)]^{2+}$ and iodide[8h] requires an explanation. Under room temperature conditions this reaction is a simple decomposition with the liberation of free $L'H_4$. The instability of the $[L'^{\Delta\Delta}Fe(II)]^{2+}$ in solution may not allow a clean redox reaction. If one assumes the slow release of free Fe(II) ion from $[L'^{\Delta\Delta}Fe(II)]^{2+}$ at a lower temperature, then its reaction with iodide to produce Fe(III) ion violates the standard redox chemistry between Fe(III) and iodide. By contrast, when iodine is used as the oxidant, the reaction product,

Scheme 2. Induced Electron Transfer Reaction between Iodine and **2**

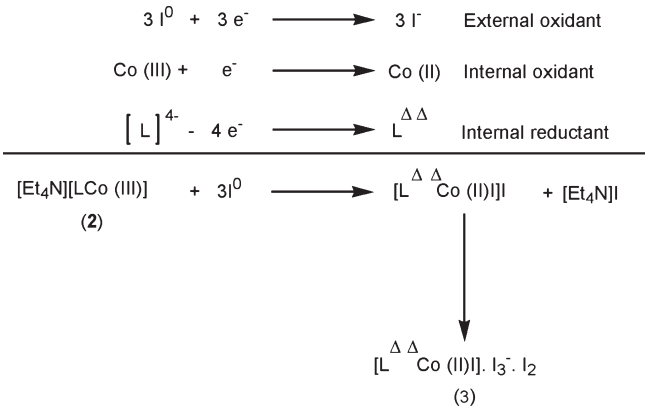

$[L^{\Delta\Delta}Fe(II)-I]^+$, reported by us is a penta-coordinated species that differs from the tetra-coordinated $[L'^{\Delta\Delta}Fe(II)]^{2+}$ ion. Thus, these two seemingly similar ions are expected to differ in redox chemistry. The difference in the chemistry between the penta-coordinated and tetra-coordinated species is not surprising. In this context, the formation of **3** can be conceived of as a rare, induced, electron-transfer reaction, which has precedent in cobalt chemistry.[22] The iodine used in this reaction acts as an external oxidant that provokes the electron transfer between Co(III) and the porphyrinogen anion (L^{4-}) in **2**. The four electrons released as a result of the oxidation of L^{4-} to $L^{\Delta\Delta}$ are shared by one internal oxidant, Co(III), and by three external oxidants, of iodine, to yield the products, $[L^{\Delta\Delta}Co(II)-I]^+[I]^-$ and $[Et_4N]^+[I]^-$, which in the presence of an excess of iodine leads to the formation of the isolable solid, $[L^{\Delta\Delta}Co(II)-I]^+ (I_3)^- (I_2)$ (**3**) (Scheme 2).

Structural Details. Oak Ridge thermal ellipsoid plot (ORTEP) and perspective diagrams of the cobalt porphyrinogen framework of $[LCo(III)]^-$ and $[L^{\Delta\Delta}Co(II)I]^+$ are shown in Figure 2 and in the Supporting Information, Figure S9. The crystallographic data and selected bond distances and angles for the two structures are provided in Tables 1 and 2, respectively. Complex **2** formed as a racemic twin crystal, as determined by the Twin RotMax routine in PLATON. The data were twinned by incorporation of the TWIN instruction in SHELXL. This complex contains one major component, as indicated by the batch scale factor (BASF) of 0.52. In a tetracoordinated environment, as defined by the four pyrrole nitrogens, $[LCo(III)]^-$ was nearly planar in structure with no significant intermolecular contacts. The two structures are distinguished by the differences in the CoN bond distance of the macrocycle core. As expected, the CoN bond distance is significantly greater for the metal center possessing a lower oxidation state, $(CoN)_{av} = 1.907$ (2) Å in octaethylporphyrinogen (L′) coordinated with Co(II),[8b] that is, $[LCo(II)]^{2-}$, compared with $(CoN)_{av} = 1.869$ (2) Å in $[LCo(III)]^-$. In the case of $[L'Co(III)]^-$,

(22) (a) Taube, H. *Electron Transfer Reaction of Complex Ions in Solution*; Academic Press: New York and London, 1970. (b) Stiefel, E. I.; Chianelli, R. R. Nitrogen Fixation; Müller A., Newton, W. E., Eds.; Plenum Press: New York, 1983; pp 341. (c) Cohen, S. S.; Stiefel, E. I. *Inorg. Chem.* **1985**, *24*, 4657. (d) Sarkar, S.; Ansari, M. A. *Chem. Commun.* **1986**, 324. (e) Chandrasekaran, J.; Ansari, A. M.; Sarkar, S. *J. Less-Common Met.* **1987**, *134*, L23. (f) Ansari, A. M.; Chandrasekharan, J.; Sarkar, S. *Inorg. Chem.* **1988**, *27*, 763.

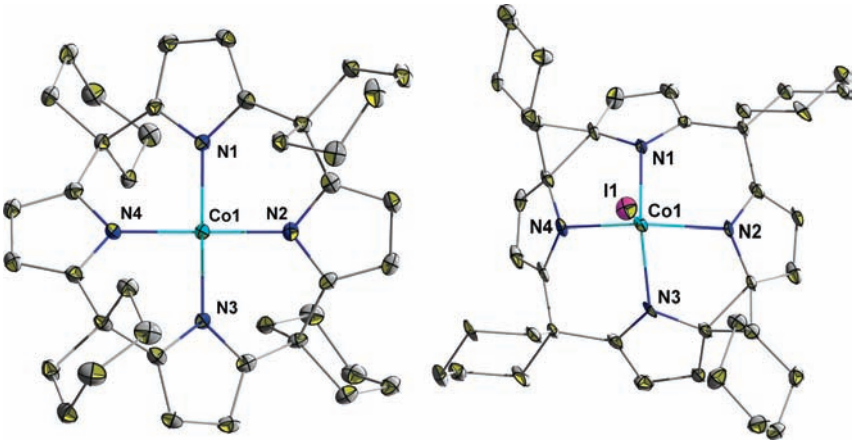

Figure 2. Structure of the cobalt porphyrinogen frameworks in $[LCo(III)]^-$ (**2**) (left) and $[L^{\triangle\triangle}Co(II)-I]^+$ (**3**) (right), with thermal ellipsoid drawn at 50% probability level ; hydrogen atoms, solvent molecule, as well as counterions are omitted for clarity. Colors: cyan, Co; blue, N; gray, C; pink, I.

Table 2. Selected Crystallographic Metric Parameters of Cobalt Porphyrinogens [a]

1[b]		**2**		**3**	
		Distances/Å			
Co(1)−N(1)	1.911(2)	Co(1)−N(1)	1.866 (2)	Co(1)−N(1)	2.084 (2)
Co(1)−N(2)	1.904 (2)	Co(1)−N(2)	1.864 (2)	Co(1)−N(2)	2.160 (2)
Co(1)−N(1′)	1.911 (2)	Co(1)−N(4)	1.879 (2)	Co(1)−N(4)	2.140 (2)
Co(1)−N(2′)	1.904 (2)	Co(1)−N(3)	1.869 (2)	Co(1)−N(3)	2.095 (2)
N(1)−C(1)	1.375 (4)	N(1)−C(1)	1.393 (2)	N(1)−C(1)	1.307 (2)
N(1)−C(4)	1.379 (3)	N(1)−C(4)	1.381 (2)	N(1)−C(4)	1.455 (2)
N(2)−C(6)	1.380 (3)	N(2)−C(6)	1.397 (2)	N(2)−C(6)	1.436 (2)
N(2)−C(9)	1.383 (4)	N(2)−C(9)	1.385 (2)	N(2)−C(9)	1.308 (2)
C(1)−C (9′)	2.511 (2)	C (4)−C (6)	2.476 (2)	C (4)−C (6)	1.579 (2)
C(6′)−C(4′)	2.456 (2)	C(9) −C (11)	2.453 (2)	C (9)−C (11)	2.435 (2)
C(1′)−C (9)	2.511 (3)	C(14)−C(16)	2.433 (2)	C(14)−C (16)	1.570 (2)
C(6)−C (4)	2.456 (2)	C(19)−C(1)	2.443 (2)	C (19)−C (1)	2.419 (2)
		Angle/deg			
N1−Co1−N2′	90.2 (1)	N1−Co1−N2	89.22 (1)	N1−Co1−N2	78.87 (1)
N2′−Co1−N1′	89.67 (1)	N2−Co1−N3	90.35 (1)	N2−Co1−N3	86.52 (1)
N1′−Co1−N2	90.21 (1)	N3−Co1−N4	90.32 (1)	N3−Co1−N4	78.66 (1)
N2−Co1−N1	89.7(1)	N4−Co1−N1	90.11 (1)	N4−Co1−N1	87.31 (1)
N1−Co1−N1′	177.0 (1)	N1−Co1−N3	179.44 (1)	N1−Co1−N3	137.10 (1)
N2−Co1−N2′	175.5 (1)	N2−Co1−N4	179.07 (1)	N2−Co1−N4	140.25 (1)

[a] Atom numbering scheme provided in Supporting Information, Figure S9. [b] For detail structural information of **1** see ref 8b.

its countercation, lithium, is coordinated to the pyrrole ring in η^4 fashion with two THF molecules, but the $[LCo(III)]^-$ ion is isolated from its countercation, Et_4N^+. (Supporting Information, Figure S1).

The distance between α carbons of the two adjacent pyrroles $(C_\alpha-C_\alpha)_{av}$ in $[LCo(III)]^-$ was 2.45 Å, indicating that porphyrinogen was in the fully reduced form. The bond distances between the two α carbons of the two adjacent pyrroles in $[L^{\triangle\triangle}Co(II)-I]^+$ were 1.579 Å (2) and 1.570 Å (2) suggesting the oxidation of the macrocycle. The observed $C_\alpha-C_\alpha$ bond distances are within the single bond distance and similar to the previously reported complex, $[L^{\triangle\triangle}Fe(II)-I](FeCl_4)$ by Nocera et al.[8h] The initial double-saddle-shaped conformation of the $[L]^{4-}$ core (displaced out of the N4 plane by the cobalt atom by only 0.058 Å (2)) changes to a bowl conformation, in which the central Co(II) atom is displaced from the N4 plane by 0.65 Å (3). The axial coordination sites around the central metal are filled by the hydrogen atoms of the cyclohexyl ring in the reduced metallomacrocycle, whereas in the oxidized form, the displacement of the metal center from the N4 plane causes axial binding of the iodide ion, producing a distorted square pyramidal geometry. However, all Co−N bond distances in the free $[L^{\triangle\triangle}Co(II)-I]^+$ entity are significantly shorter than those in the previously reported polynuclear counteranion, $[L^{\triangle\triangle}Co(II)-Cl][Cu_4Cl_5]$, complex. This result indicates that the interaction of the $[Cu_4Cl_5]^-$ counteranion cluster with the cobalt porphodimethene moiety drastically affects the structural parameters.[8e] Our approach to the synthesis of a stable bis(cyclopropane) moiety in the cobalt-porphyrinogen system is unique, as it has no influence with the exception of the electrostatic cation−anion interaction in the complex.

Compound **3** contains one I_3^- and one neutral iodine molecule in the lattice. The $[L^{\triangle\triangle}Co(II)-I]^+$ unit is distributed along the *ab* plane, and the polymeric $\cdots I_3^- \cdots I_2 \cdots I_3^- \cdots I_2 \cdots$ zigzag network is stacked between two planes of porphodimethenes. The ordered symmetric chains are located along the *b* axis in the crystal. The interaction between the I_3^- ions and the neutral iodine

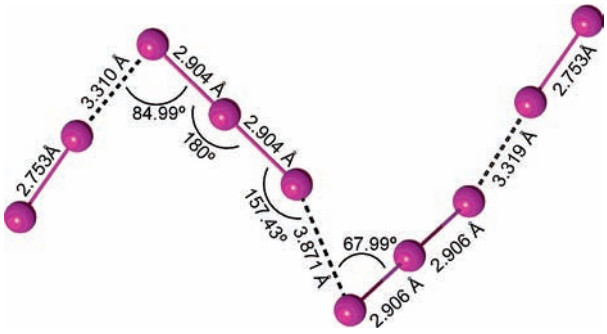

Figure 3. View of the polymeric zigzag chain of interacting planar I_3^- ions with I_2 molecules.

molecules is shown in Figure 3 (see also Supporting Information, Figures S2 and S3). The slightly bent nature of I_3^- is typical of iodine-doped metallophthalocyanines.[23] The I−I bond distance of 2.753 Å for the I_2 molecule in the lattice is slightly larger than the 2.715 (6) Å[24] for pure iodine in the solid state. The I···I distance of 3.319 (2) Å between the terminal I of the I_3^- ion and the I of the I_2 molecule within the polyiodide chains is slightly shorter than the intermolecular distance of 3.50 Å[24] found in pure iodine. These values indicate a strong interaction between the I_2 and I_3^- moieties in the chain. The $[L^{\triangle\triangle}Co(II)-I]^+$ unit in the crystal form pseudo−monodimensional chains, which are aligned along the *b* axis of the crystal, and the mean planes of the porphodimethene rings are parallel to the *ac* plane. The intermolecular ring distance between the two neighboring porphodimethene units is greater than 11 Å, which rules out any ring $\pi-\pi$ interaction. At various temperatures (room to high), **3** did not show any conductivity, which rules out the presence of a non-integral, formal oxidation state, despite the systematic array of crystal packing.

Electrochemistry. Figure 4 shows the cyclic voltammogram of $[Et_4N][LCo(III)]$ in acetonitrile. Reversible metal-centered reduction occurred at $E_{1/2} = -0.50$ V (vs Ag/AgCl electrode), as verified by the linear plot of the cathodic and anodic current versus $\nu^{1/2}$ (scan rate, ν = 100−1000 mV S^{1-}) (Supporting Information, Figure S4). The redox reaction at positive potential displayed two irreversible oxidation reactions. Quantification of the number of electrons involved in these reactions is difficult and non-informative as the irreversibility suggests that the electro-generated species is unstable in the CV time scale, which dissipated responding chemical reactions. Porphyrinogens are predicted to respond normally to a pair of successive two-electron oxidations. Use of different solvents in electrochemical reactions allows for fine-tuning of the reversible $[LCo(III)]^-/[LCo(II)]^{2-}$ potential change. In oxygen-donor solvents (like DMSO and THF), the cobaltic state is more stable than it is in nitrogen-donor solvents (like MeCN, DMF). Again, in non-coordinating solvents, like dichloromethane, the Co(III) state is unstable $E_{1/2} = -0.6$ V (vs Ag/AgCl), and oxidation occurs in one step (Supporting Information, Figure S5). Therefore, in dichloromethane, $[LCo(III)]^-$ functions as a one-step, four−equivalent hole reservoir in a porphyrinogen framework (considering $C_\alpha-C_\alpha$ bond formation as a two-electron process), but in coordinating solvents, it is a successive two-step process. $[Et_4N]_2[LCo(II)]$ and $[Et_4N][LCo(III)]$ were stable in a basic medium, but decomposed in an acidic medium,[25] possibly because of protonation of the ligand. In solvents like MeCN, DMF, and DMSO, complexes are more stable than in non-coordinating solvents, as observed from electrochemical study. The solvent-dependent variation in the value of the redox potential for this complex may be due to interaction of the solvent molecules, which act as donor ligands, with the central cobalt ion. However, the possible rotation of the peripheral cyclohexyl groups of the porphyrinogen in **2** in solution may perturb the relative energy level, as observed for the $[LFe(III)]^-$ complex anion.[8i] This may explain the solvent dependency of the formal redox potential of **2**. The solvent-dependent perturbation of the relative energy level will also influence the magnetic behavior of **2** in solution, as shall be described later. The four-electron-oxidized product, $[L^{\triangle\triangle}Co(II)-I](I_3)(I_2)$, showed a metal-centered, reversible-reduction reaction at $E_{1/2} = -0.72$ V (vs Ag/AgCl), suggesting the accessibility of the Co(I) state. A quantitative difference in redox behavior was observed between the iron- and cobalt-porphyrinogens in a particular solvent system. In MeCN, the $[LCo(III)]^-/[LCo(II)]^{2-}$ couple appeared at −0.5 V versus Ag/AgCl instead of at −0.82 V versus Ag/AgCl for $[LFe(III)]^-/[LFe(II)]^{2-}$. Therefore, the well-defined, two-step, two-electron oxidation reactions proceeded more readily in the case of $[L^{\triangle\triangle}Co(II)]^{2+}/[LCo(III)]^-$ compared with the corresponding iron complex[8i] (Supporting Information, Figure S5). There was a reversible peak due to I_3^-/I^- couple with the absence of any ligand oxidation process. This result is expected for the fully oxidized ligand, porphodimethene, in **3**.

Electronic Structure. On the basis of the DFT (B3LYP) theoretical framework, the ground-state electronic structure was calculated to determine the energies and compositions of the molecular orbitals (MOs) using the geometry of the crystal structure of **2**. The assignment of the type of each MO was made on the basis of its composition and by visual inspection of its three-dimensional representation. Selected frontier molecular orbitals and their relative energies were computed and are shown in Figure 5. For the system with two unpaired electrons (compound **2**), the spin-unrestricted calculation showed a sufficient energy difference between the α and β spinors because of spin contamination. The pairs of spinors with antiparallel spin and similar spatial extent for the metal-based functions were correlated (Figure 5). Similar electronic correlations have been made recently with iron-porphyrinogen.[8g] The molecular orbital that is predominantly populated with $d_{x^2-y^2}$ is fully vacant and is highly destabilized. The next two low-energy, single-occupied molecular orbitals are mostly populated with d_{xy} and d_{yz}. The remaining two metal d orbitals are confined to deeply buried molecular orbitals that are fully occupied. The intense color of $[LCo(III)]^-$ arises from the bands at

(23) Janczak, J. *Inorg. Chem.* **2003**, *42*, 3549 and references therein.
(24) Van Bolhius, F.; Kostner, B; Migchelsen, P. *Acta Crystallogr.* **1967**, *23*, 90.
(25) (a) Hegetschweiler, K.; Kuppert, D.; Huppert, J.; Straka, M.; Kaupp, M. *J. Am. Chem. Soc.* **2004**, *21*, 6728. (b) Cowley, R. E.; Bontchev, R. P.; Sorrell, J.; Sarracino, O.; Feng, Y.; Wang, H.; Smith, J. M. *J. Am. Chem. Soc.* **2007**, *129*, 2424.

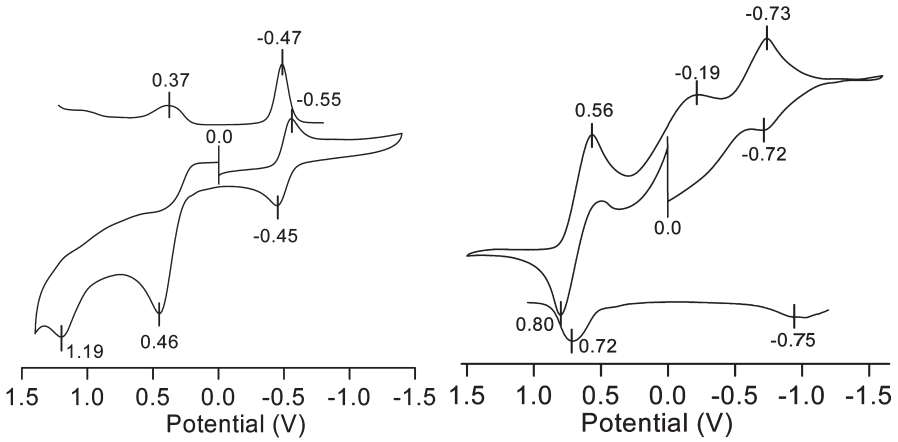

Figure 4. Cyclic voltammogram and differential pulse polarographic signal of 1 mM acetonitrile solution of $[Et_4N][LCo(III)]$ (**2**) (left) and $[L^{\Delta\Delta}Co(II)-I](I_3)(I_2)$ (**3**) (right) and 0.1 M Bu_4NClO_4: CV was recorded at a sweep rate of 100 mV/s and DPP at a sweep rate of 20 mV/s.

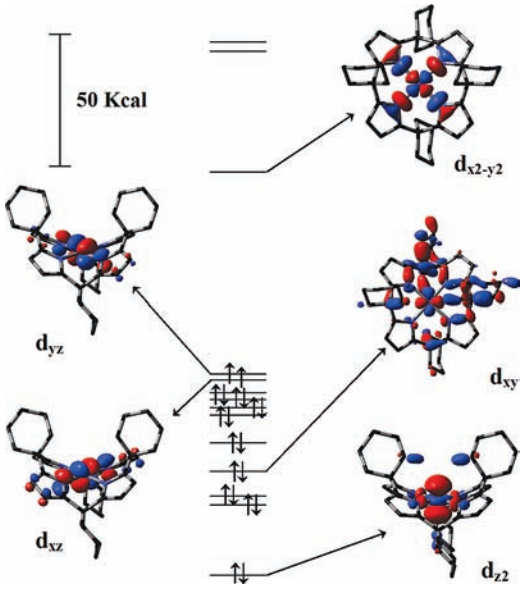

Figure 5. Pictorial representative molecular orbital diagram for $[LCo(III)]^-$ using the DFT method at the B3LYP/LanL2DZ level spin unrestricted single point calculation. An isovalue of 0.02 was used.

473 (ε = 3831) and 734 (ε = 4476) nm that dominate the absorption profile. A shoulder at 575 nm was also observed. The ligand-to-metal character of these charge transfer bands concurs with the reducing nature of the $[L]^{4-}$ ligand and the presence of an oxidizing Co(III) center. The featureless profiles of both $[LCo(II)]^{2-}$ and $[L^{\Delta\Delta}Co(II)-I]^+$ support this ligand-to-metal charge transfer (LMCT) assignment, because the reduction of the metal and the oxidation of the ligand would cause the LMCT to blue-shift in the UV region. In the present study, charge transfer absorption was not observed for these compounds in this range. In solution, $[Et_4N][LCo(III)]$ was brown, while its derivatives in other oxidation states were pale in color. Figure 6 (left) shows the absorption spectrum of $[LCo(III)]^-$. It has been well documented that cyclopropane unit formation is parallel to the aromatization of porphyrinogen to porphyrins, which causes the LMCT to undergo a bathochromic shift in the UV region. The solution of $[L^{\Delta\Delta}Co(II)-I](I_3)(I_2)$ (Figure 6, right) showed absorption peaks at 524 nm due to the presence of a free iodine molecule and at 293 and 363 nm, indicative of I_3^-.

Magnetic Properties. The magnetic susceptibilities of **1**, **2**, and **3** were measured in the solid state at temperatures ranging between 300 and 5 K. The magnetic moment values were measured in solution[26] to ascertain any solid state or solvent effects. The temperature-dependent diamagnetic contribution of the porphyrinogen ring and the diamagnetic contribution from the I_3^- and I_2 were calculated from Pascal's constants.[27] The corrected magnetic moment values of **1**, **2**, and **3** at 300 K were 3.98, 3.44, and 3.90 μ_B, respectively. Compound **1** followed Curie–Weiss behavior in the temperature range of 300–5 K, and a value of 3.98 μ_B at 300 K is expected for the Co(II) d^7 system. The solid-state magnetic moment value of **2** indicates a triplet ground state with an orbital contribution. The magnetic susceptibility followed the Curie–Weiss law over the temperature range of 300–50 K. Below 50 K, the magnetic susceptibility clearly deviated from Curie–Weiss behavior (Supporting Information, Figures S6–S8). Interestingly, the solution magnetic moment value of **2**, as measured by Evan's method, was 2.49 in DCM, and in DMF it was 2.98 μ_B The difference between solvents may not be due to solvent coordination, as the bulky porphyrinogen around Co(III) may prevent any solvent effects. This hypothesis can readily be tested by comparing the donor properties of DCM and DMF, as evaluated based on the observed magnetic moment values. The weak DCM may not result in splitting greater than that caused by the better donor (DMF) in axial coordination in **2**. Depending on the polarity of the solvent, the spatial orientation of the peripheral cyclohexyl moieties may influence the relative molecular orbital in **2**, which in turn may be reflected in the variation in magnetic moment in solution. The existence of various conformers in solution is known.[8i]

Electron Spin Resonance. The X–band ESR spectrum of **1** showed superhyperfine interaction of Co(II)[28] (d^7,

(26) Evans, D. F. *J. Chem. Soc.* **1959**, 2003.
(27) (a) Earnshaw, A. In *Introduction to Magnetochemistry*; Academic Press: London, 1968; pp 4–8. (b) Mulay, L. N. In Theory and Applications of Molecular Diamagnetism; Mulay, L. N., Boudreaux, E. A., Eds.; Wiley-Interscience: New York, 1976; Chapter 5.3.
(28) Collins, T. J.; Powell, R. D.; Slebodnick, C.; Uffelman, E. S. *J. Am. Chem. Soc.* **1991**, *113*, 8419.

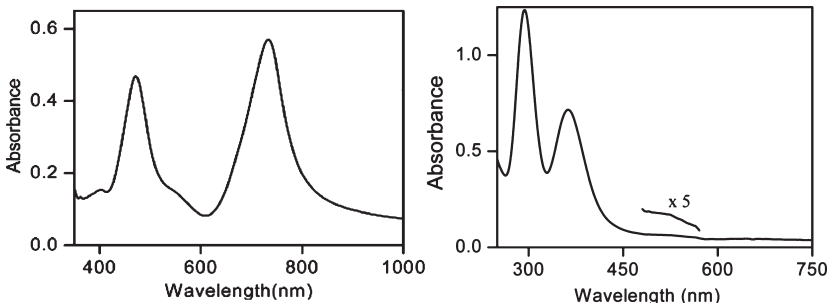

Figure 6. UV−visible spectra: 10^{-4} M dichloromethane solution of $[Et_4N][LCo(III)]$ (**2**) (left) $[L^{\triangle\triangle}Co(II)-I]$ (I_3) (I_2) (**3**) (right).

$S = 3/2$) with the pyrrole nitrogen atoms of the porphyrinogen ring in DCM at 120 K (Supporting Information, Figure S10). A featureless ESR spectrum ($\langle g \rangle = 2.006$) of the powdered sample of **3** at room temperature was obtained (Supporting Information, Figure S11). The formation of superoxide radicals during oxidation of **1** to **2** in air was difficult to verify because of its instability and the strong electron paramagnetic resonance (EPR) signal that originated from cobalt. Therefore, we used a chemical method to verify the formation of superoxide radical ions during the reaction, namely, the nitroblue tetrazolium (NBT) formazan assay.[29] A colorless, aqueous solution of NBT was layered over a DCM solution of $[Et_4N][LCo(III)]$ in an argon atmosphere. The argon blanket was then removed to allow air to come in contact with the solution. Immediately, a blue color developed[8j] in the aqueous layer and also was evident in the DCM solution. Thus, oxygen interacts with cobalt(II)porphyrinogen according to the reaction shown in Scheme 3. The outer-sphere, electron-transfer reaction mechanism is also supported by the smooth oxidation of **1** to **2** using $[Cp_2Fe][PF_6]$ as the oxidant.

Summary and Conclusions. We have shown a facile route for the synthesis of cobalt(III) porphyrinogen and its ligand based oxidized product. An intensive examination of the interaction of atmospheric oxygen with Co(II) porphyrinogens showed two distinct reaction pathways: a metal-centered one-electron oxidation of **1** to cobalt(III) porphyrinogen as reported here; and, a ligand-centered two-electron oxidation to $[L^{\triangle}Co(II)]$, as reported earlier. The difference in reactivity is attributed to the cationic counterions in these complexes. The clean reaction of metal-centered oxidation of **1** to **2** in 80% yield was observed when the lithium cation that participates in η−binding with the pyrollyl ring of the porphyrinogen was replaced with the non-interacting tetraalkylammonium cation. Furthermore, **2** reacts with iodine in a rare, induced, electron-transfer reaction that uses Co(III) as the internal oxidant, iodine as the external oxidant, and coordinated porphyrinogen as the internal reductant.

Scheme 3. Reaction of Molecular Oxygen with Cobalt(II)porphyrinogen

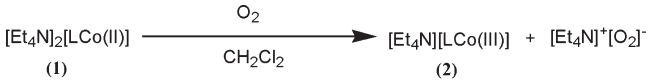

Acknowledgment. D.B. thanks IIT Kanpur for a Senior Teaching Fellowship, S.M. and K.P. to CSIR, New Delhi, India, for SRF, and S.S. to the DST, New Delhi for funding the project.

Supporting Information Available: X-ray crystallographic files (CIF), crystal packing of **3**, cyclic voltammograms of **1** in different solvents, magnetic plot of **1**, **2**, and **3** and solid state EPR spectra of **1** and **3**. This material is available free of charge via the Internet at http://pubs.acs.org.

(29) (a) Lombard, M.; Houe′e-Levin, C.; Touati, D.; Fontecave, M.; Niviére, V. *Biochemistry* **2001**, *40*, 5032. (b) Beauchamp, C.; Fridovich, I. *Anal. Biochem.* **1971**, *44*, 276.